Real-space observation of ligand holes in $SrFeO_3$

An anomalously high valence state of a transition-metal element sometimes shows up in oxide compounds. In such systems, holes tend to occupy mainly the ligand *p* orbitals, giving rise to interesting physical properties such as superconductivity in cuprates and rich magnetic phases in ferrates.

$SrFeO_3$ is an archetypal tetravalent ferrate compound, in which, at least formally, four electrons occupy the Fe 3*d* orbitals. It forms the perovskite-type structure with the cubic space group $Pm\bar{3}m$ (Fig. 1(a)) and exhibits metallic conductivity [1]. The local symmetry at the Fe site is $m\bar{3}m$. Each Fe atom is surrounded by an O_6 regular octahedron without Jahn-Teller distortion, where the 3*d* orbitals are split into the lower-lying triplet (t_{2g}) and the higher-lying doublet (e_g). The high-spin state of $3d^4$ corresponds to the $t_{2g}^3 e_g^1$ electron configuration, which causes some anisotropy in the valence electron density. However, previous X-ray photoelectron spectroscopy and X-ray absorption spectroscopy measurements suggest that the ground state consists of mixed $3d^4$ and $3d^5\underline{L}$ ($\underline{L}$: ligand hole) states [2,3]. In the extreme limit of the $3d^5\underline{L}$ state, the electron density around the Fe site should be spherical because of the $t_{2g}^3 e_g^2$ electron configuration.

Although the ligand holes in the crystal have been observed by spectroscopy measurements [2,3], no one has ever seen where the ligand holes exist in real space. To observe the spatial distribution of the holes, the measurement with high-wavevector (Q) resolution is indispensable. In this study, we observe the valence electron density distribution of $SrFeO_3$ by electron density analysis using state-of-the-art synchrotron X-ray diffraction (XRD).

XRD experiments were performed at SPring-8 **BL02B1**. A He-gas-blowing device was employed to cool the crystal to 30 K. The X-ray wavelength was $\lambda = 0.31020$ Å. A two-dimensional detector CdTe PILATUS, which had a dynamic range of ~10^7, was used to record the diffraction pattern. The intensities of Bragg reflections with the interplane distance $d > 0.28$ Å were collected. A core differential Fourier synthesis (CDFS) method [4] was used to extract the valence electron density distribution around each atomic site. [Kr], [Ar], and [He] type electron configurations were regarded as core electrons for Sr, Fe, and O atoms, respectively.

Figure 1(b) shows the valence electron density distribution of $SrFeO_3$ at 30 K. No valence electron density larger than $3e$/Å^3 is observed around the Sr site, which is consistent with the Sr^{2+} ($5s^0$) state. In contrast, valence electrons are observed around the Fe and O sites, as shown by yellow iso-density surfaces. An orange iso-density surface for higher electron distribution is observed only around the Fe site, which is clearly distinct from a sphere: there are six hollow holes toward the six ligand oxygens.

To quantify the anisotropy of the valence electron density $\rho(\boldsymbol{r})$ around the Fe site, the density at a distance r = 0.2 Å from the Fe nucleus is shown by a color map on a sphere (Fig. 2(a)). The maximum and minimum electron densities are present along the <111> and <100> axes, respectively. Figures 2(b) and 2(c) show surface color maps of $\rho(\theta,\phi)$ for the calculated electron density considering the high-spin $3d^4$ and $3d^5$ states for an isolated Fe ion, respectively. In the case of $3d^4$, we assume that an

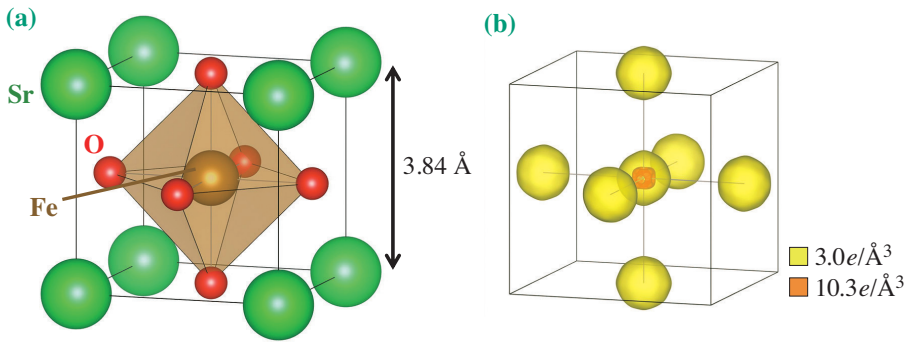

Fig. 1. **(a)** Crystal structure and **(b)** valence electron density distribution of $SrFeO_3$ at 30 K. Yellow and orange iso-density surfaces show electron-density levels of 3.0 and 10.3e/Å^3, respectively.

electron occupies each e_g orbital with a probability of 1/2. A clear anisotropy is observed in the $3d^4$ state, in contrast to the completely isotropic electron density in the $3d^5$ state. By comparing the CDFS results and simulations, the number of Fe 3*d* electrons is estimated to be N_e = 4.64(8), which is consistent with the previous reports of X-ray absorption spectroscopy measurement (N_e = 4.7) [3].

Since the corresponding valence of Fe obtained by the CDFS analysis was 3.36(8), the oxygen valence is estimated to be –1.79(3), which deviates from the ideal closed-shell value of –2. That is, the valence electron density distribution around the O site should not be isotropic. Figure 2(d) shows a color map of the electron density $\rho(\theta,\phi)$ at a distance r = 0.40 Å from the O nucleus, obtained from the CDFS analysis. The observed $\rho(\theta,\phi)$ has some anisotropy, which differs from the isotropic behavior of an ideal O^{2-} ion (Fig. 2(e)). While the highest electron density exists toward the surrounding four Sr atoms, the lowest electron density is observed in the [100] direction toward Fe. These results suggest the existence of ligand holes accommodated in the O $2p_\sigma$ — Fe 3*d* antibonding σ* orbital. The distribution of ligand holes around the O site was captured for the first time by the CDFS analysis [5].

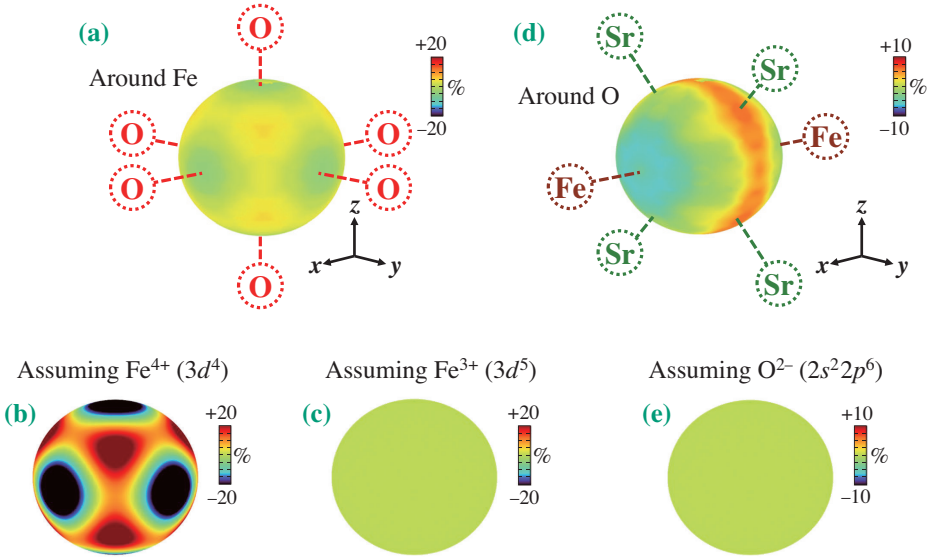

Fig. 2. Color map of the electron density **(a)** at a distance r = 0.2 Å from the Fe nucleus and **(b)** at a distance r = 0.4 Å from the O nucleus. Color maps of the calculated direction dependence of electron density for the **(c)** Fe^{4+} $3d^4$, **(d)** Fe^{3+} $3d^5$ and **(e)** O^{2-} $2s^2sp^6$ states assuming isolated Fe and O atoms. The color bar scale is represented by $\frac{[\rho(\theta,\phi)-N_e/4\pi]}{N_e/4\pi}\times 100(\%)$. N_e is the number of valence electrons.

Shunsuke Kitou* and Taka-hisa Arima

Department of Advanced Materials Science,
The University of Tokyo

*Email: kitou@edu.k.u-tokyo.ac.jp

References

[1] J. B. MacChesney *et al.*: J. Chem. Phys. **43** (1965) 1907.
[2] M. Abbate *et al.*: Phys. Rev. B **65** (2002) 165120.
[3] A. E. Bocquet *et al.*: Phys. Rev. B **45** (1992) 1561.
[4] S. Kitou *et al.*: Phys. Rev. Res. **2** (2020) 033503.
[5] *S. Kitou, M. Gen, Y. Nakamura, K. Sugimoto, Y. Tokunaga, S. Ishiwata and T. Arima: Adv. Sci.* ***10*** *(2023) 2302839.*